Chaos, Solitons and Fractals 140 (2020) 110163

Contents lists available at ScienceDirect

Chaos, Solitons and Fractals

Nonlinear Science, and Nonequilibrium and Complex Phenomena

journal homepage: www.elsevier.com/locate/chaos

Occurrence of backward bifurcation and prediction of disease transmission with imperfect lockdown: A case study on COVID-19

Sk Shahid Nadim*, Joydev Chattopadhyay

Agricultural and Ecological Research Unit, Indian Statistical Institute, Kolkata 700 108, India

ARTICLE INFO

Article history:
Received 1 May 2020
Revised 15 July 2020
Accepted 26 July 2020
Available online 17 August 2020

Keywords:
COVID-19
Mathematical model
Imperfect lockdown
Backward bifurcation
Parameter estimation
Prediction

ABSTRACT

The outbreak of COVID-19 caused by SARS-CoV-2 is spreading rapidly around the world, which is causing a major public health concerns. The outbreaks started in India on March 2, 2020. As of April 30, 2020, 34,864 confirmed cases and 1154 deaths are reported in India and more than 30,90,445 confirmed cases and 2,17,769 deaths are reported worldwide. Mathematical models may help to explore the transmission dynamics, prediction and control of COVID-19 in the absence of an appropriate medication or vaccine. In this study, we consider a mathematical model on COVID-19 transmission with the imperfect lockdown effect. The basic reproduction number, R_0, is calculated using the next generation matrix method. The system has a disease-free equilibrium (DFE) which is locally asymptotically stable whenever $R_0 < 1$. Moreover, the model exhibits the backward bifurcation phenomenon, where the stable DFE coexists with a stable endemic equilibrium when $R_0 < 1$. The epidemiological implications of this phenomenon is that the classical epidemiological requirement of making R_0 less than unity is only a necessary, but not sufficient for effectively controlling the spread of COVID-19 outbreak. It is observed that the system undergoes backward bifurcation which is a new observation for COVID-19 disease transmission model. We also noticed that under the perfect lockdown scenario, there is no possibility of having backward bifurcation. Using Lyapunov function theory and LaSalle Invariance Principle, the DFE is shown globally asymptotically stable for perfect lockdown model. We have calibrated our proposed model parameters to fit daily data from India, Mexico, South Africa and Argentina. We have provided a short-term prediction for India, Mexico, South Africa and Argentina of future cases of COVID-19. We calculate the basic reproduction number from the estimated parameters. We further assess the impact of lockdown during the outbreak. Furthermore, we find that effective lockdown is very necessary to reduce the burden of diseases.

1. Introduction

An outbreak of 2019 coronavirus disease (COVID-19) has resulted in 30,90,445 confirmed cases and 2,17,769 deaths as of April 30, 2020 according to WHO [1]. The outbreak was first taken place in Wuhan, China, in December 2019, with the majority of early cases reported in the city. Coronaviruses are single-stranded, positive-sense RNA viruses belonging to the Coronaviridae family [2]. It has been confirmed that 27 people have been infected due to viral pneumonia, including seven critically ill cases [3], and this epidemic has drawn tremendous attention worldwide. It causes variety of symptoms, including dry cough, fever, weakness, trouble breathing, and bilateral lung infiltration, close to those caused by SARS-CoV and MERS-CoV infections [4,5]. Severe outbreaks occur in so many countries and the disease continues to spread worldwide [1]. On 11 March 2020, WHO declared Novel Coronavirus Disease (COVID-19) outbreak as a pandemic. SARS-CoV-2 is strongly associated with two serious, bat-derived acute respiratory syndrome-like coronaviruses. It is transmitted through human-to-human transmission through droplets or through direct contact [6,7]. On January 30, 2020, after H1N1 (2009), polio (2014), Ebola in West Africa (2014), Zika (2016), and Ebola in the Democratic Republic of Congo (2019), the WHO announced the COVID-19 epidemic to be the sixth public health emergency of international concern. Since the first discovery and identification of coronavirus in 1965, there are three major outbreaks occurred due to coronaviruses and the outbreak was called 'Severe Acute Respiratory Syndrome' (SARS) outbreak (2003) in China [8]. Saudi Arabia suffered from 'Middle East Respiratory Syndrome' (MERS) outbreak (2012) [9] and South Korea (2015) [10].

The Indian government reported that on 30 January 2020 in the state of Kerala, India's first case of Coronavirus disease 2019, when a Wuhan university student traveled back to the state [11]. On 24

* Corresponding author.
E-mail address: nadimskshahid@gmail.com (S.S. Nadim).

https://doi.org/10.1016/j.chaos.2020.110163
0960-0779/

March, the Government of India ordered a 21-day nationwide lockdown restricting the movement of India's entire 1.3 billion population as a preventive measure against India's 2020 coronavirus pandemic. The lockdown was imposed when approximately 500 confirmed positive coronavirus cases were reported in India. As the end of the lockdown period reached, it recommended an extension of the lockdown by state governments and other advisory committees. On 14 April 2020, Prime Minister extended the nationwide lockdown to May 3, with a conditional relaxation after April 20, for those regions where the spread was contained. In addition to the lock-down, India's Ministry of Health and Family Welfare (MOHFW) has introduced various individual hygiene steps such as frequent hand washing, social distancing, mask use, avoiding touching eyes, nose, or mouth, etc [12]. COVID-19 is an effectively spreading pandemic across the world and an unprecedented threat to the community's health care, economy and lifestyle. For all, there is a huge worry as to how long this condition can continue and whether the epidemic can be handled.

We also study the cases of Mexico, South Africa and Argentina as the lockdown was carried out partially or in a less severe form in these countries. In February 2020 the virus was confirmed to reach Mexico. However, two cases of COVID-19 reported by the National Council of Science and Technology (CONACYT) in the states of Nayarit and Tabasco by mid-January 2020. A national lockdown was announced in Mexico, starting on 23 March 2020. As of July 13, there had been 275,003 confirmed cases of COVID-19 in Mexico and 32,796 reported deaths [13]. Health Ministery reported on 5 March 2020 that the virus spread to South Africa, with the first patient being a male citizen who tested positively while returning from Italy. On 23 March, a national lockdown was announced in South Africa, starting on 26 March 2020. As of 9 July 2020, there were 238,339 confirmed cases and 3720 people died. The virus had been confirmed to have spread to Argentina on 3 March 2020. A total of 90,693 people were confirmed to have been infected as of 9 July 2020, and 1720 people were known to have died from the virus. On 19 March in Argentina, a nationwide lockdown was declared until 31 March. Later the government extended the lockdown until mid-April, then June 28, 2020.

Mathematical modeling based on differential equations may provide a comprehensive mechanism for the dynamics of the disease and also to test the efficacy of the control strategies to reduce the burden of the disease. Several studies were performed using real-life data from the affected countries and analyzed various features of the outbreak as well as assess the impact of intervention such as lockdown approaches to suppress the outbreak in the concerned countries [3,14–19]. There are also some mathematical works investigating the effect of the lock-down on the dynamics of COVID-19 transmission in India.

Recently lockdown measure has been used successfully to control COVID-19 spread. The aim of this study is to investigate the qualitative effect of the imperfect lockdown on the spread of disease dynamics. To achieve this goal, a mathematical model for COVID-19 with the lockdown is proposed and analyzed. In this model, we implemented the imperfect lockdown, which means that the lockdown susceptible population also gets infected during the lockdown period by unnotified infected individuals. We looked at India's situation during the outbreak period and fitted our model with the newly daily cases reported from March 14th, 2020 to April 19th, 2020. We also looked at the situation of Mexico, South Africa and Argentina during the outbreak period and fitted our model with the new daily cases reported for a certain outbreak period. We are providing a short-term prediction for India, Mexico, South Africa and Argentina of future cases of COVID-19 using the estimated parameters for the period March 14, 2020, to May 21, 2020, March 23, to July 9, March 17, to July 9, and March 14, to July 9, respectively. For the above-mentioned period we aslo estimate the basic reproduction number. It is common for classical epidemic models that a basic reproduction number is a threshold in the context that if the basic reproduction number is greater than one, a disease will persist, and dies out if it is less than one. In this case, for imperfect lockdown, the basic reproduction number does not represent the required elimination effort; rather, the effort at the turning point is described by the value of the critical parameter. Thus, to obtain thresholds for disease control it is necessary to identify backward bifurcations. However this backward bifurcation phenomenon is not new in epidemic model. In the past, the existence of a backward bifurcation and the conditions for its emergence in epidemic models have been studied extensively. The problem of identifying the causes of backward bifurcation for the spread of some emerging and re-emerging diseases studied by A.B.Gumel in some standard deterministic models [20]. Garba et al. have been studying backward bifurcations in dynamics of dengue transmission with imperfect vaccine [21]. There investigation is the backward bifurcation phenomenon can be removed by substituting the associated standard incidence function with a mass action incidence. Influence of backward bifurcation on interpretation of reinfection in a model of epidemic tuberculosis studied by Singer et al. [22]. Backward bifurcation of a disease model with saturated treatment function was also studied [23]. Although this is not a new phenomenon, it is new in the COVID model due to imperfect nature of lockdown efficacy. The effect of lockdown on the disease burden is also studied. The paper is organized as follows: Our proposed mathematical model which incorporates the lockdown of susceptible individuals and imperfect lockdown efficacy is described in Section (2). The model is analyzed specifically for the existence of backward bifurcation in Section (3). In Section (4) we fitted our model to daily new cases. We provided a short-term prediction for India, Mexico, South Africa and Argentina of future cases of COVID-19 in the Section (5). The impact of lockdown and control strategies is studied in Section (6). Finally in Section (7) we discuss the results from our study.

2. Model formulation

Mathematical models were previously identified for the spread of infectious diseases [24,25]. We consider a compartmental deterministic modeling approach to explain the mechanism for transmitting disease. We introduced a variant that incorporates some of COVID-19 key epidemiological properties such as lockdown, isolation, etc. The total human population denoted by $N(t)$ is divided into six mutually exclusive sub-populations of susceptible human $S(t)$, lockdown population $L(t)$, exposed individuals $E(t)$, unnotified infected individuals $I(t)$, hospitalized or isolated individuals $J(t)$ and recovered populations $R(t)$, so that so that $N(t) = S(t) + L(t) + E(t) + I(t) + J(t) + R(t)$. The lockdown is nothing but a percentage of the susceptible population that has been quarantined at home for a certain period of time. The flow diagram of the proposed model is shown in Fig. 1. The susceptible individuals is generated by recruiting people by birth or immigration into the community at a constant rate Π. In this model, lockdown refers to the separation of susceptible populations from the entire susceptible populations during the lockdown phase, while hospitalization or isolation describes the separation of individuals infected with COVID-19 when the population is notified of symptomatic infection. Here we consider $\frac{1}{\psi}$ as a lockdown period, l is the lockdown success rate. The population is reduced after infection, which can be transmitted at a rate $\frac{\beta I}{N-J}$ (the force of infection of human) through effective contact with an un-notified infected individuals. We consider $0 < r < 1$, the lockdown efficacy, $\frac{1}{\gamma}$ as the incubation period. We assume the recovery rate of un-notified and hospitalized individuals as τ_1 and τ_2 respectively. Our model incor-

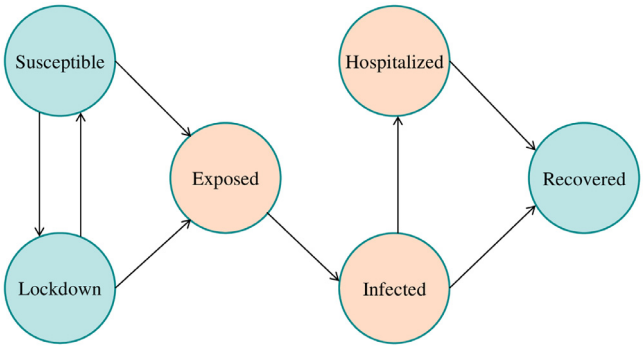

Fig. 1. Flow diagram of the model (2.1).

porates some demographic effects by assuming a disease-induced death rate δ of hospitalized individuals and natural death rate μ of each six sub-population. We develop the following compartmental model for COVID-19 outbreak based on these assumptions:

$$\begin{aligned}
\frac{dS}{dt} &= \Pi + \psi L - \frac{\beta SI}{N-J} - (\mu + l)S \\
\frac{dL}{dt} &= lS - \frac{r\beta LI}{N-J} - (\mu + \psi)L, \\
\frac{dE}{dt} &= \frac{\beta SI}{N-J} + \frac{r\beta LI}{N-J} - (\gamma + \mu)E, \\
\frac{dI}{dt} &= \gamma E - (\eta + \tau_1 + \mu)I, \\
\frac{dJ}{dt} &= \eta I - (\tau_2 + \delta + \mu)J, \\
\frac{dR}{dt} &= \tau_1 I + \tau_2 J - \mu R.
\end{aligned} \tag{2.1}$$

All the parameters and their biological interpretation are given in Table 1 respectively.

3. Mathematical analysis of model (2.1)

3.1. Positivity and boundedness of the solution for the model (2.1)

Since the model (2.1) represent different human population, all the variables of are nonnegative for all $t \geq 0$. Let

$$\Omega = \left\{ (S, L, E, I, J, R) \in \mathbb{R}^6_+ | S + L + E + I + J + R \leq \frac{\Pi}{\mu} \right\}$$

We first claim the following result.

Theorem 3.1. *Solutions of the model (2.1) with positive initial data will remain positive for all time $t > 0$ and the biologically feasible region $\Omega \in \mathbb{R}^6_+$ is positively invariant and globally attracting for system (2.1).*

Proof. The system (2.1) can be written as follows

$$\frac{dx}{dt} = f(x) \tag{3.1}$$

where $x = (x_1, x_2, x_3, x_4, x_5, x_6) = (S, L, E, I, J, R)$ and $f(x) = (f_1(x), ., f_6(x))$ denotes the right hand side functions. It is very obvious that for every $j = 1, \ldots, 6$, $f_j(x) \geq 0$ if $x \in [0, \infty)^6$ and $x_j = 0$. Since the human populations, N(t) are positive, therefore the right-hand side of (3.1) is locally Lipschitz in Ω. So, by Theorem A.4 in [28], model (2.1) has a unique solution in Ω. Adding all the equations of the model (2.1), total human populations satisfy the following equations,

$$\frac{dN}{dt} = \Pi - \mu N - \delta J \leq \Pi - \mu N$$

Since $\frac{dN}{dt} \leq \Pi - \mu N$, it follows that $\frac{dN}{dt} \leq 0$ if $N \geq \frac{\Pi}{\mu}$. Thus, by using standard comparison theorem [29], it can be shown that $N \leq N(0)e^{-\mu t} + \frac{\Pi}{\mu}(1 - e^{-\mu t})$. In particular, $N(t) \leq \frac{\Pi}{\mu}$ if $N(0) \leq \frac{\Pi}{\mu}$. Thus, the region Ω is positively-invariant. Further, if $N(0) > \frac{\Pi}{\mu}$, then either the solution enters Ω in finite time, or $N(t)$ approaches $\frac{\Pi}{\mu}$ asymptotically. Hence, the region Ω attracts all solutions in $\mathbb{R}_+{}^6$. □

3.2. Basic reproduction number and local stability of disease-free equilibrium (DFE)

The basic reproduction number R_0 is a threshold value that is epidemiologically significant and determines the potential of an infectious disease to enter a population. To obtain the basic reproduction number R_0 of the system (2.1), we apply the next generation matrix approach. The system has a disease-free equilibrium given by

$$\varepsilon_0 = \left(\frac{\Pi(\mu + \psi)}{\mu(\mu + \psi + l)}, \frac{\Pi l}{\mu(\mu + \psi + l)}, 0, 0, 0, 0 \right).$$

The infected compartments of the model (2.1) consist of ($E(t)$, $I(t)$, $J(t)$) classes. Following the next generation matrix method, the matrix F of the transmission terms and the matrix, V of the transition terms calculated at ε_0 are,

$$F = \begin{pmatrix} 0 & \frac{\beta(\mu+\psi+rl)}{(\mu+\psi+l)} & 0 \\ 0 & 0 & 0 \\ 0 & 0 & 0 \end{pmatrix},$$

$$V = \begin{pmatrix} \gamma + \mu & 0 & 0 \\ -\gamma & \eta + \tau_1 + \mu & 0 \\ 0 & -\eta & \tau_2 + \delta + \mu \end{pmatrix}.$$

So, the next generation matrix FV^{-1} is,

$$FV^{-1} = \begin{pmatrix} \frac{\beta\gamma(\mu+\psi+rl)}{(\mu+\gamma)(\eta+\tau_1+\mu)(\mu+\psi+l)} & \frac{\beta(\mu+\psi+rl)}{(\eta+\tau_1+\mu)(\mu+\psi+l)} & 0 \\ 0 & 0 & 0 \\ 0 & 0 & 0 \end{pmatrix},$$

Calculating the dominant eigenvalue of the next generation matrix FV^{-1}, we obtain the basic reproductive number as follows [30,31]

$$R_0 = \frac{\beta\gamma(\mu + \psi + rl)}{(\mu + \gamma)(\eta + \tau_1 + \mu)(\mu + \psi + l)} \tag{3.2}$$

The basic reproduction number R_0 is defined as the expected number of secondary cases generated by one infected individual during its lifespan as infectious in a fully susceptible population. The basic reproduction number R_0 of (2.1) given in (3.2).

Using Theorem 2 in [31], the following result is established.

Lemma 3.1. *The disease-free equilibrium ε_0 of system (2.1) is locally asymptotically stable whenever $R_0 < 1$, and unstable whenever $R_0 > 1$.*

3.3. Existence of endemic equilibrium

We are now exploring the existence of endemic equilibrium. Let $\varepsilon^* = (S^*, L^*, E^*, I^*, J^*, R^*)$ be any endemic equilibrium of system (2.1). Let us denote

$$k_1 = \mu + l, k_2 = \mu + \psi, k_3 = \gamma + \mu, k_4 = \eta + \tau_1 + \mu, k_5 = \tau_2 + \delta + \mu.$$

Further, the force of infection be

$$\lambda_h^* = \frac{\beta I^*}{N^* - J^*} \tag{3.3}$$

By setting the right equations of system (2.1) equal to zero, we have

$$S^* = \frac{\Pi(r\lambda_h^* + k_2)(\lambda_h^* + k_1)}{(\lambda_h^* + k_1)((r\lambda_h^* + k_2)(\lambda_h^* + k_1) - l\psi)}, L^* = \frac{\Pi l}{((r\lambda_h^* + k_2)(\lambda_h^* + k_1) - l\psi)},$$
$$E^* = \frac{\lambda_h^* S^*(r\lambda_h^* + k_2 + rl)}{k_3(r\lambda_h^* + k_2)}, I^* = \frac{\lambda_h^* S^* \gamma(r\lambda_h^* + k_2 + rl)}{k_3 k_4(r\lambda_h^* + k_2)}, J^* = \frac{\lambda_h^* S^* \gamma\eta(r\lambda_h^* + k_2 + rl)}{k_3 k_4 k_5(r\lambda_h^* + k_2)}$$
$$R^* = \frac{\lambda_h^* S^*(r\lambda_h^* + k_2 + rl)(\tau_1\gamma k_5 + \tau_2 + \eta\gamma)}{\mu k_3 k_4 k_5(r\lambda_h^* + k_2)} \tag{3.4}$$

Substituting the expression in (3.4) into (3.3) shows that the non-zero equilibrium of the model (2.1) satisfy the following quadratic equation, in terms of λ_h^*:

$$A\lambda_h^{*2} + B\lambda_h^* + C = 0 \tag{3.5}$$

where

$$A = r(\mu k_4 k_5 + \mu\gamma k_5 + \mu\eta\gamma + \tau_1\gamma k_5 + \tau_2\eta\gamma)$$
$$B = \mu r k_3 k_4 k_5 + m(k_2 + rl) - \beta\gamma\mu r k_5 \tag{3.6}$$
$$C = \mu k_3 k_4 k_5(k_2 + l)(1 - R_0)$$

The endemic equilibrium of the model (2.1) can be obtained by solving for λ_h^* from (3.5), and substituting the values of λ_h^* into the expressions in (3.4). The quadratic Eq. (3.5) can be analyzed for the possibility of multiple endemic equilibria when $R_0 < 1$. Note that the coefficient A is always positive of the quadratic Eq. (3.5) and C is positive or negative if R_0 is less or greater than unity. Hence, the following result is established.

Theorem 3.2. *The model (2.1) has (i) a unique endemic equilibrium if $C < 0$ iff $R_0 > 1$;*

(ii) a unique endemic equilibrium if ($B < 0$ and $C = 0$) or $B^2 - 4AC = 0$;

(iii) two endemic equilibria if $C > 0$, $B < 0$ and $B^2 - 4AC > 0$;

(iv) no endemic equilibrium otherwise.

Therefore, it is obvious from Case (i) of Theorem (3.2) that the model (2.1) has a unique EEP (of the form ε^*) whenever $R_0 > 1$. In addition, Case (iii) of Theorem (3.2) implies the possibility of backward bifurcation where stable DFE coexists with a stable endemic equilibrium whenever the basic reproduction number R_0 is less than unity. The epidemiological importance of the phenomenon of backward bifurcation is that the classical requirement of having $R_0 < 1$ is, although necessary, not sufficient for disease elimination. In this case the elimination of disease would depend on the initial sizes of the model's sub-populations. Thus, the occurrence of backward bifurcation in the dynamics of a disease transmission complicates its effective control.

In order to check the possibility of backward bifurcation in (2.1), the discriminant $B^2 - 4AC$ of the quadratic (3.5), is set to zero and the result solved for the critical value (denoted by R_0^c) of R_0. This gives:

$$R_0^c = 1 - \frac{B^2}{4Ak_3k_4(\mu + \psi + l)}$$

from which we have seen that backward bifurcation occurs for values of R_0 such that $R_0^c < R_0 < 1$. We explore the details analysis of backward bifurcation in the next section. This phenomenon is illustrated numerically by simulation of the model (2.1) (See the Fig. 2).

3.4. Backward bifurcation analysis

For disease transmission models, having the associated basic reproduction number, denoted by R_0, less than unity is necessary condition for disease control. However, this condition may not always be sufficient for the backward bifurcation phenomenon, where a stable endemic equilibrium co-exists with a stable disease-free equilibrium for $R_0 < 1$. Clearly, this phenomenon has significant public health consequences, as it makes the classical requirement of the associated basic reproduction number being less than unity to be necessary, but not sufficient to eradicate the disease.

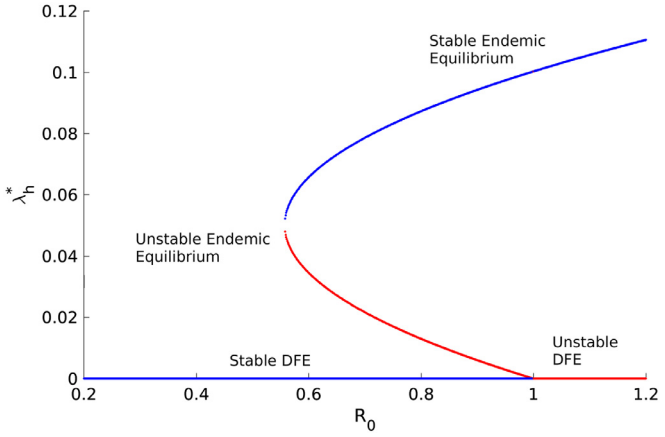

Fig. 2. Backward bifurcation diagram for the force of infection (λ_h^*) of the model (2.1). Using the parameter values: $\psi = 0.000246$, $\mu = 0.0049$, r=0.09, $\gamma = 0.0016$, $\eta = 0.0159$, β=5.905, $\tau_1 = 0.0101$, $\tau_2 = 0.0094$, $\delta = 0.0332$, l=0.09.

In this section, we explore the phenomenon of backward bifurcation in system (2.1). First, we execute bifurcation analysis by using the center manifold theorem [32] (see the Theorem Appendix A.1 in **Appendix A**). Let $x = (x_1, x_2, x_3, x_4, x_5, x_6)^T = (S, L, E, I, J, R)^T$. Thus, the model (2.1) can be re-written in the form $\frac{dx}{dt} = f(x)$, with $f(x) = (f_1(x), f_6(x))$, as follows:

$$\begin{aligned}
\frac{dx_1}{dt} &= f_1 = \Pi + \psi x_2 - \frac{\beta x_1 x_4}{x_1 + x_2 + x_3 + x_4 + x_6} - (\mu + l)x_1 \\
\frac{dx_2}{dt} &= f_2 = lx_1 - \frac{r\beta x_2 x_4}{x_1 + x_2 + x_3 + x_4 + x_6} - (\mu + \psi)x_2, \\
\frac{dx_3}{dt} &= f_3 = \frac{\beta x_1 x_4}{x_1 + x_2 + x_3 + x_4 + x_6} + \frac{r\beta x_2 x_4}{x_1 + x_2 + x_3 + x_4 + x_6} - (\gamma + \mu)x_3, \\
\frac{dx_4}{dt} &= f_4 = \gamma x_3 - (\eta + \tau_1 + \mu)x_4, \\
\frac{dx_5}{dt} &= f_5 = \eta x_4 - (\tau_2 + \delta + \mu)x_5, \\
\frac{dx_6}{dt} &= f_6 = \tau_1 x_4 + \tau_2 x_5 - \mu x_6.
\end{aligned} \tag{3.7}$$

The Jacobian of the system (3.7) at the DFE ε_0 is given as,

$$J_{\varepsilon_0} = \begin{pmatrix}
-(\mu + l) & \psi & 0 & -\frac{\beta(\mu+\psi)}{(\mu+\psi+l)} & 0 & 0 \\
l & -(\mu + \psi) & 0 & -\frac{r\beta l}{(\mu+\psi+l)} & 0 & 0 \\
0 & 0 & -(\gamma + \mu) & \frac{\beta(\mu+\psi+rl)}{(\mu+\psi+l)} & 0 & 0 \\
0 & 0 & \gamma & -(\eta + \tau_1 + \mu) & 0 & 0 \\
0 & 0 & 0 & \eta & -(\tau_2 + \delta + \mu) & 0 \\
0 & 0 & 0 & \tau_1 & \tau_2 & -\mu
\end{pmatrix},$$

Choose β as the bifurcation parameter, then setting $R_0 = 1$ gives

$$\beta = \beta^* = \frac{(\mu + \gamma)(\eta + \tau_1 + \mu)(\mu + \psi + l)}{\gamma(\mu + \psi + rl)} \tag{3.8}$$

The system (3.7) at the DFE ε_0 evaluated for $\beta = \beta^*$ has a simple eigenvalue with zero real part, and all other eigenvalues have negative real part. We therefore apply the Center Manifold Theorem in order to analyze the dynamics of (3.7) near $\beta = \beta^*$.

The Jacobian of (3.7) at $\beta = \beta^*$, denoted by $J_{\varepsilon_0}|\beta = \beta^*$ has a right eigenvector (corresponding to the zero eigenvalue) given by $w = (w_1, w_2, w_3, w_4, w_5, w_6)^T$, where

$$w_1 = -\left(\frac{\mu}{l}w_2 + \frac{\beta(\mu + \psi + rl)}{l(\mu + \psi + l)}w_4\right), w_2 = w_2 > 0,$$
$$w_3 = \frac{\beta(\mu + \psi + rl)}{(\mu + \gamma)(\mu + \psi + l)}w_4,$$

$$w_4 > 0, w_5 = \frac{\eta}{\tau_2+\delta+\mu}w_4,$$
$$w_6 = \frac{\tau_1(\tau_2+\delta+\mu)+\tau_2\eta}{\mu(\tau_2+\delta+\mu)}w_4. \quad (3.9)$$

Similarly, from $J_{\varepsilon_0}|\beta=\beta^*$, we obtain a left eigenvector $v=(v_1,v_2,v_3,v_4,v_5,v_6)^T$ (corresponding to the zero eigenvalue), where

$$v_1=0, v_2=0, v_3>0, v_4=\frac{\beta(\mu+\psi+rl)}{(\mu+\psi+l)(\eta+\tau_1+\mu)}v_3,$$
$$v_5=0, v_6=0. \quad (3.10)$$

We calculate the following second order partial derivatives of f_i at the disease-free equilibrium ε_0 to show the existence of a backward bifurcation and obtain

$$\frac{\partial^2 f_3}{\partial x_4\partial x_1}=\frac{(1-r)l\mu\beta}{\Pi(\mu+\psi+l)}, \frac{\partial^2 f_3}{\partial x_4\partial x_2}=-\frac{(1-r)\mu(\mu+\psi)\beta}{\Pi(\mu+\psi+l)}, \frac{\partial^2 f_3}{\partial x_4\partial x_3}=-\frac{\mu(\mu+\psi+rl)\beta}{\Pi(\mu+\psi+l)},$$

$$\frac{\partial^2 f_3}{\partial x_1\partial x_4}=\frac{(1-r)l\mu\beta}{\Pi(\mu+\psi+l)}, \frac{\partial^2 f_3}{\partial x_2\partial x_4}=-\frac{(1-r)(\mu+\psi)\mu\beta}{\Pi(\mu+\psi+l)}, \frac{\partial^2 f_3}{\partial x_3\partial x_4}=-\frac{(\mu+\psi+rl)\mu\beta}{\Pi(\mu+\psi+l)},$$

$$\frac{\partial^2 f_3}{\partial x_4\partial x_4}=-\frac{2(\mu+\psi+rl)\mu\beta}{\Pi(\mu+\psi+l)}, \frac{\partial^2 f_3}{\partial x_6\partial x_4}=-\frac{(\mu+\psi+rl)\mu\beta}{\Pi(\mu+\psi+l)}, \frac{\partial^2 f_3}{\partial x_4\partial x_6}=-\frac{\mu(\mu+\psi+rl)\beta}{\Pi(\mu+\psi+l)}, \quad (3.11)$$

Now we calculate the coefficients a and b defined in Theorem 4.1 [32] of CastilloChavez and Song as follow

$$a=\sum_{k,i,j=1}^{6} v_k w_i w_j \frac{\partial^2 f_k(0,\beta^*)}{\partial x_i\partial x_j}$$
$$=v_3w_4\Big[r((\mu+\psi)w_2-l(w_1+w_3+w_4+w_6)) \quad (3.12)$$
$$-(\mu+\psi)(w_2+w_3+w_4+w_6)+lw_1\Big]\frac{\beta\mu}{\Pi(\mu+\psi+l)}$$

and

$$b=\sum_{k,i=1}^{6} v_k w_i \frac{\partial^2 f_k(0,0)}{\partial x_i\partial\beta}=v_3v_4\frac{(\mu+\psi+rl)}{(\mu+\psi+l)}>0. \quad (3.13)$$

Since the coefficient b is always positive, system (2.1) undergoes backward bifurcation at $R_0=1$, if $a>0$, namely if

$$r>\frac{(\mu+\psi)(w_2+w_3+w_4+w_6)-lw_1}{(\mu+\psi)w_2-l(w_1+w_3+w_4+w_6)} \quad (3.14)$$

We have established the following conclusion.

Theorem 3.3. *System (2.1) undergoes a backward bifurcation at $R_0=1$ whenever the inequality (3.14) holds.*

Furthermore, it should be noted that for the case when lockdown susceptible individuals do not acquire infection during lockdown period (i.e., $r=0$), the bifurcation coefficient a becomes

$$a=-v_3w_4\Big[(\mu+\psi)(w_2+w_3+w_4+w_6)-lw_1\Big]\frac{\beta\mu}{\Pi(\mu+\psi+l)}<0.$$

Thus, since $a<0$ in this case, it follows from Theorem 4.1 of [32] that the model (2.1) will not exhibit backward bifurcation if $r=0$. In other words, this study shows that the backward bifurcation property of the model (2.1) arises due to the infection of lockdown susceptible individuals in lockdown period. This result is consistent with Theorem (3.4) (where it was shown that the DFE of the model (2.1) with $r=0$ is globally-asymptotically stable).This result is associated with theorem (3.4), where DFE of the model (2.1) with $r=0$ has been shown to be globally-asymptotically stable.

Since $a<0$ and $b>0$ at $\beta=\beta^*$, therefore using the Remark 1 of the Theorem 4.1 stated in [32], a transcritical bifurcation occurs at $R_0=1$ whenever r=0 (See the Fig. 3). Hence, the following result is established.

Lemma 3.2. *The unique endemic equilibrium ε^* at $r=0$ is locally asymptotically stable if $R_0>1$.*

3.4.1. Non-existence of backward bifurcation

In this section we discussed in which the backward bifurcation phenomenon of the model (2.1) can be lost. We consider the model (2.1) with a perfect lockdown efficacy against infection (so that, $r=0$). In this case, the coefficients A, B and C of the quadratic Eq. (3.5) reduce to $A=0$, $B>0$ and $C\geq 0$ whenever $R_0^*=R_0|_{r=0}\leq 1$. Thus, for this case, the quadratic Eq. (3.5) has one solution ($\lambda_h^*=\frac{-C}{B}$). Therefore, the model (2.1) with a perfect lockdown has no positive endemic equilibrium whenever $R_0<1$. This eliminates the possibility of backward bifurcation in this case because backward bifurcation requires at least two endemic equilibriums whenever $R_0^*<1$ [21]. Also, it can be seen that in the case where r=0, the DFE ε_0 of the model (2.1) is globally-asymptotically stable (GAS) under some certain conditions, as shown below.

Setting $r=0$ in the model (2.1) gives the following reduced model:

$$\frac{dS}{dt}=\Pi+\psi L-\frac{\beta SI}{N-J}-(\mu+l)S$$
$$\frac{dL}{dt}=lS-(\mu+\psi)L,$$

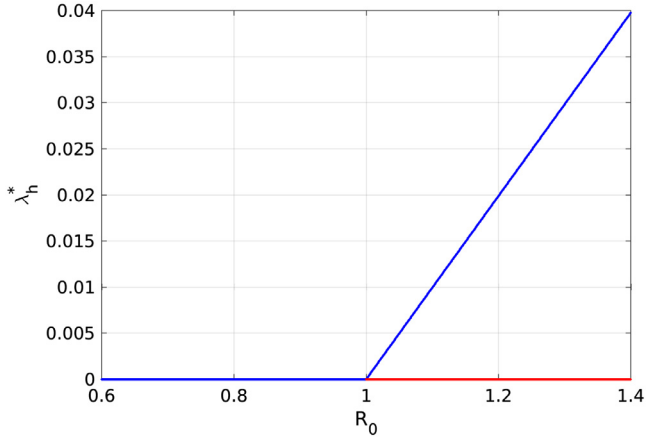

Fig. 3. Transcritical bifurcation for the force of infection (λ_h^*) of the model (2.1). Using the parameter values: $\psi=0.000246$, $\mu=0.0049$, r=0, $\gamma=0.0016$, $\eta=0.0159$, $\tau_1=0.0101$, β=0.5.905, $\tau_2=0.0094$, $\delta=0.0332$, l=0.09.

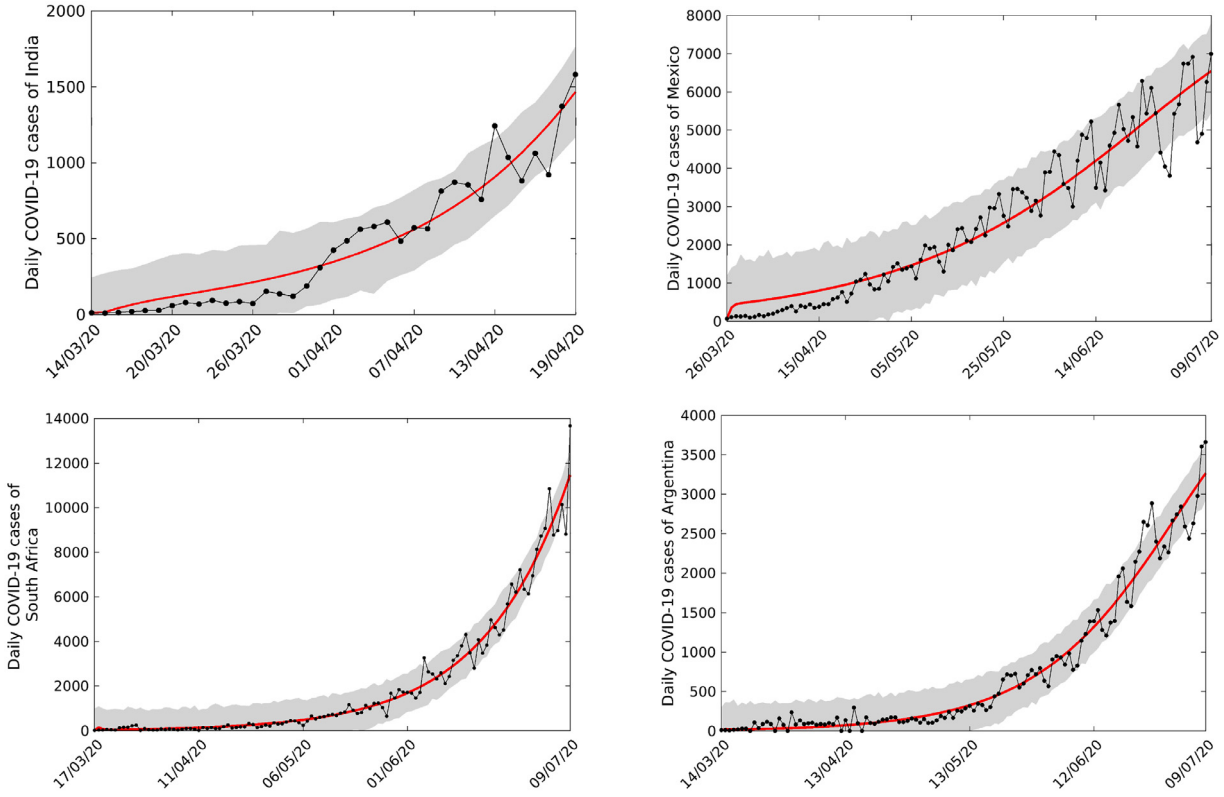

Fig. 4. Model (2.1) fitting to newly daily notified COVID-19 cases in India, Mexico, South Africa and Argentina. Daily notified cases are depicted in black curve with circles and red curve is the solution of model (2.1). Grey shaded region is the 95% confidence region. (For interpretation of the references to colour in this figure legend, the reader is referred to the web version of this article.)

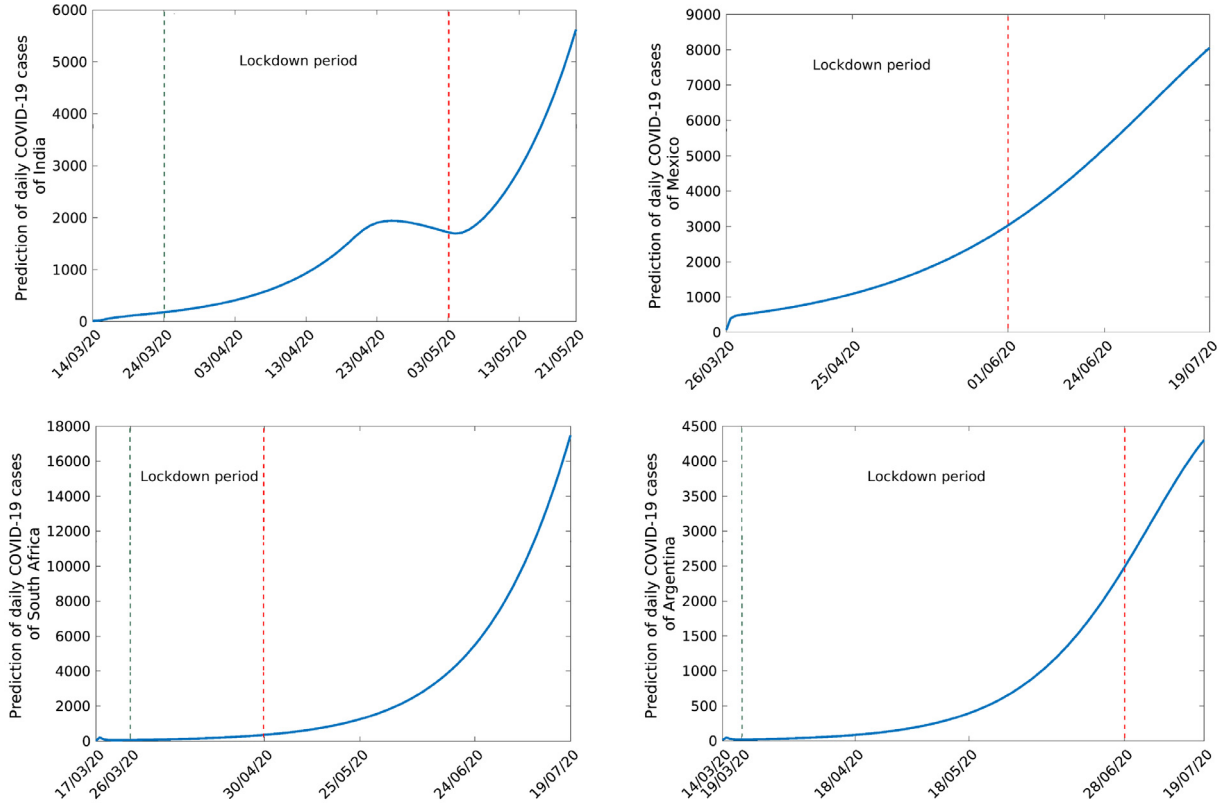

Fig. 5. The short term predictions for India India, Mexico, South Africa and Argentina. Green dotted line indicates the starting day of lockdown and the red dotted line indicates the end of the lockdown period. (For interpretation of the references to colour in this figure legend, the reader is referred to the web version of this article.)

Table 1
Model (2.1) parameters with biological interpretations.

Parameters	Biological Meaning	Value/Ranges	Reference
Π	Recruitment rate of human population	Varies over different country	-
$1/\mu$	Average life expectancy at birth	Varies over different country	[13]
β	Transmission rate of infected individuals	(0 - 200) day^{-1}	Estimated
r	Lockdown efficacy	0 - 1	Assumed
$1/\gamma$	Incubation period for COVID-19	(1 - 14) *days*	Estimated
l	Lockdown success rate	0–1	[16]
η	Rate at which Symptomatic infected become Hospitalized or Notified	(0 - 1) day^{-1}	Estimated
δ	Death rate of Hospitalized or Notified population	Varies over different country	[26]
τ_1	Recovery rate for Symptomatic infected	(0 - 1) day^{-1}	Estimated
$1/\psi$	Lockdown period	Varies over different country	[27]
τ_2	Recovery rate for Hospitalized or Notified individuals	Varies over different country	[26]

Table 2
Estimated parameter values of the model (2.1) for the countries India, Mexico, South Africa and Argentina. All data are given in the format [**Mean(95% CI)**].

Country	Estimated parameters	Values (95% confidence interval)
India	β	0.3904 (0.1973 - 0.6244)
	γ	0.1555 (0.0833 - 0.2355)
	η	0.1632 (0.0395 - 0.2739)
	τ_1	0.0101 (0.0006 - 0.0108)
Mexico	β	0.9463 (0.8258 - 1.053)
	γ	0.7657 (0.7320 - 0.9702)
	η	0.0703 (0.0450 - 0.0710)
	τ_1	0.8101 (0.6976 - 0.9686)
South Africa	β	1.5025 (0.7539 - 2.0627)
	γ	0.0842 (0.0721 - 0.0864)
	η	0.1661 (0.1511 - 0.5323)
	τ_1	0.7221 (0.1250 - 0.7726)
Argentina	β	1.1080 (0.8324 - 1.2075)
	γ	0.1182 (0.1145 - 0.1952)
	η	0.0130 (0.0086 - 0.0162)
	τ_1	0.7006 (0.5621 - 0.8643)

Table 4
Model (2.1) parameters values for India, Mexico, South Africa and Argentina.

Country	Π	μ	δ	τ_2
India	4.878×10^4	3.8905×10^{-5}	0.0332	0.1649
Mexico	4.183×10^3	3.6336×10^{-5}	0.1193	0.6102
South Africa	2.170×10^3	4.2215×10^{-5}	0.0156	0.4744
Argentina	1.257×10^3	3.5489×10^{-5}	0.0189	0.4145

Table 5
Estimated values of the basic reproduction number (R_0) for the countries India, Mexico, South Africa and Argentina.

Country	**Basic Reproduction Number (R_0)**
India	2.2519
Mexico	1.0748
South Africa	1.6907
Argentina	1.5518

$$\begin{aligned}
\frac{dE}{dt} &= \frac{\beta SI}{N-J} - (\gamma+\mu)E,\\
\frac{dI}{dt} &= \gamma E - (\eta+\tau_1+\mu)I,\\
\frac{dJ}{dt} &= \eta I - (\tau_2+\delta+\mu)J,\\
\frac{dR}{dt} &= \tau_1 I + \tau_2 J - \mu R.
\end{aligned} \tag{3.15}$$

It can be shown that the reproduction number associated with the reduced model (3.15), is given by

$$R_0^* = R_0|_{r=0} = \frac{\beta\gamma(\mu+\psi)}{(\mu+\gamma)(\eta+\tau_1+\mu)(\mu+\psi+l)}$$

The model (3.15) has a DFE $\varepsilon_{01} = (S^1, L^1, 0, 0, 0, 0)$.

Theorem 3.4. *The DFE (ε_{01}) of the reduced model (3.15), is globally asymptotically stable in Ω whenever $R_0^* \le \theta < 1$, where $\theta = \frac{\mu+\psi}{\mu+\psi+l}$.*

Proof. Consider the following Lyapunov function

$$\mathcal{D} = \left(\frac{\gamma k_2}{\theta k_3(k_2+l)}\right)E + \left(\frac{k_2}{\theta(k_2+l)}\right)I$$

We take the Lyapunov derivative with respect to t,

$$\begin{aligned}
\dot{\mathcal{D}} &= \left(\frac{\gamma k_2}{\theta k_3(k_2+l)}\right)\dot{E} + \left(\frac{k_2}{\theta(k_2+l)}\right)\dot{I}\\
&= \frac{\gamma k_2}{\theta k_3(k_2+l)}\left[\frac{\beta SI}{N-J} - k_3E\right] + \frac{k_2}{\theta(k_2+l)}[\gamma E - k_4 I]\\
&= \frac{\beta\gamma k_2}{\theta k_3(k_2+l)}\frac{SI}{N-J} - \frac{\gamma k_2}{\theta(k_2+l)}E + \frac{k_2\gamma}{\theta(k_2+l)}E - \frac{k_2k_4}{\theta(k_2+l)}I\\
&\le \frac{\beta\gamma k_2}{\theta k_3(k_2+l)}I - \frac{k_2k_4}{\theta(k_2+l)}I \text{ (Since } S \le N-J \text{ in } \Omega)\\
&= \frac{\beta\gamma k_2}{\theta k_3k_4(k_2+l)}k_4I - k_4I\\
&= k_4\left(\frac{\beta\gamma k_2}{\theta k_3k_4(k_2+l)} - 1\right)I\\
&= k_4\left(\frac{R_0^*}{\theta} - 1\right)I \le 0, \text{ whenever } R_0^* \le \theta < 1.
\end{aligned}$$

Since all the variables and parameters of the model (2.1) are non-negative, it follows that $\dot{\mathcal{D}} \le 0$ for $R_0 \le \theta$ with $\dot{\mathcal{D}} = 0$ in diseases free equilibrium. Hence, $\mathcal{D}$ is a Lyapunov function on Ω. Therefore,

Table 3
Estimated initial values of the model (2.1) for the countries India, Mexico, South Africa and Argentina. All data are given in the format [**Mean(95% CI)**].

Country	S(0)	E(0)	I(0)
India	1228552474(1218445699 – 1294102459)	1566(1485 – 8297)	20(1 – 23)
Mexico	115109620(115000170 – 115162299)	9398(7126 – 9577)	4859(2046 – 4736)
South Africa	51403188(45208819 – 54881645)	224(26 – 1506)	1748(14 – 1770)
Argentina	35414537(35053817 – 41633824)	1709(155 – 5501)	4601(62 – 4949)

Table 6
Normalized sensitivity indices of R_0 with respect to the model parameters for India, Mexico, South Africa and Argentina.

Country	β	γ	η	τ_1	l	r
India	1.0000	2.55×10^{-4}	−0.9415	−0.0583	−0.3418	0.6094
Mexico	1.0000	4.74×10^{-5}	−0.0790	−0.9201	−0.2360	0.7362
South Africa	1.0000	5.01×10^{-4}	−0.1870	−0.8130	−0.3631	0.5827
Argentina	1.0000	3.01×10^{-4}	−0.0182	−0.9817	−0.1795	0.8010

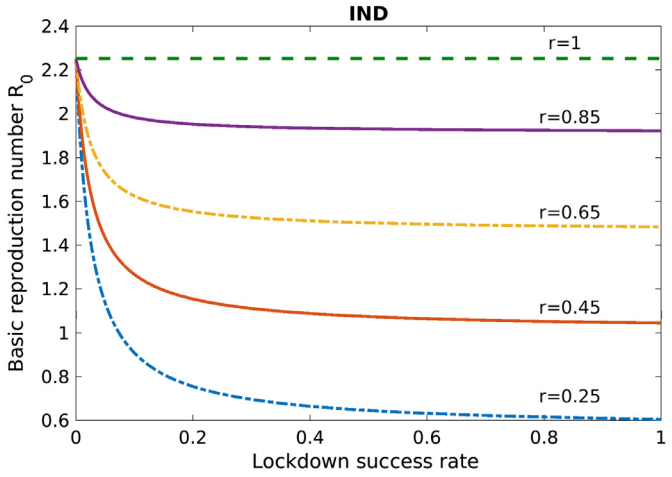

Fig. 6. Effect of lockdown success rate l on basic reproduction number R_0 for India.

followed by LaSalles Invariance Principle [33], that

$$(E(t), I(t)) \to (0, 0) \text{ as } t \to \infty \tag{3.16}$$

Since $\lim_{t\to\infty} supI(t) = 0$ (from (3.16)), it follows that, for sufficiently small $\epsilon > 0$, there exist constants $M > 0$ such that $\lim_{t\to\infty} supI(t) \le \epsilon$ for all $t > M$.

Hence, it follows that,

$$\frac{dJ}{dt} \le \eta\epsilon - k_5 J$$

Therefore using comparison theorem [29]

$$J^\infty = \lim_{t\to\infty} supJ(t) \le \frac{\eta\epsilon}{k_5}$$

So as $\epsilon \to 0$, $J^\infty = \lim_{t\to\infty} supJ(t) \le 0$

Similarly by using $\lim_{t\to\infty} infI(t) = 0$, it can be shown that

$$J_\infty = \lim_{t\to\infty} infJ(t) \ge 0$$

Thus, it follows from above two relations

$$J_\infty \ge 0 \ge J^\infty$$

Hence $\lim_{t\to\infty} J(t) = 0$

Similarly, it can be shown that

$$\lim_{t\to\infty} R(t) = 0, \lim_{t\to\infty} S(t) = \frac{\Pi(\mu+\psi)}{\mu(\mu+\psi+l)}, \lim_{t\to\infty} L(t) = \frac{\Pi l}{\mu(\mu+\psi+l)},$$

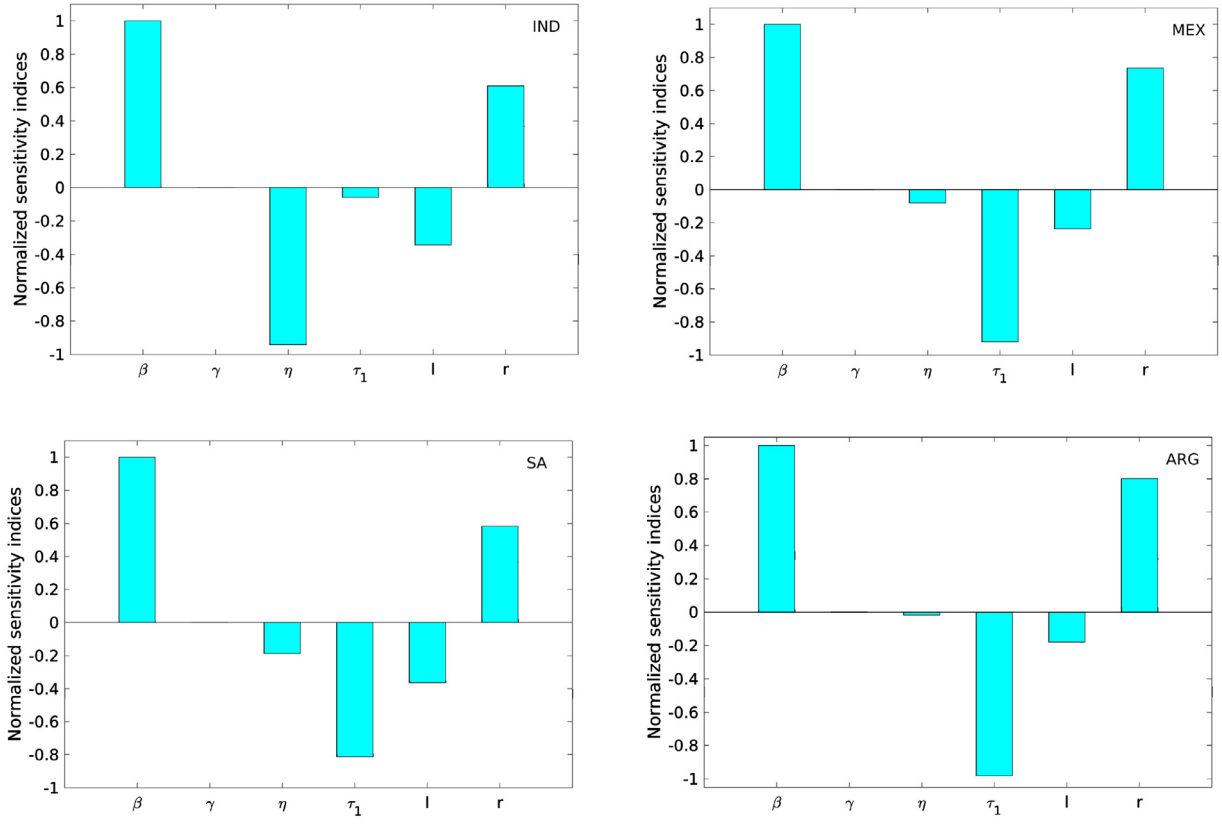

Fig. 7. Normalized sensitivity indices of R_0 with respect to parameters of the model (2.1) for India(IND), Mexico(MEX), South Africa(SA) and Argentina(ARG). Parameter values are taken from Tables 2 and 4.

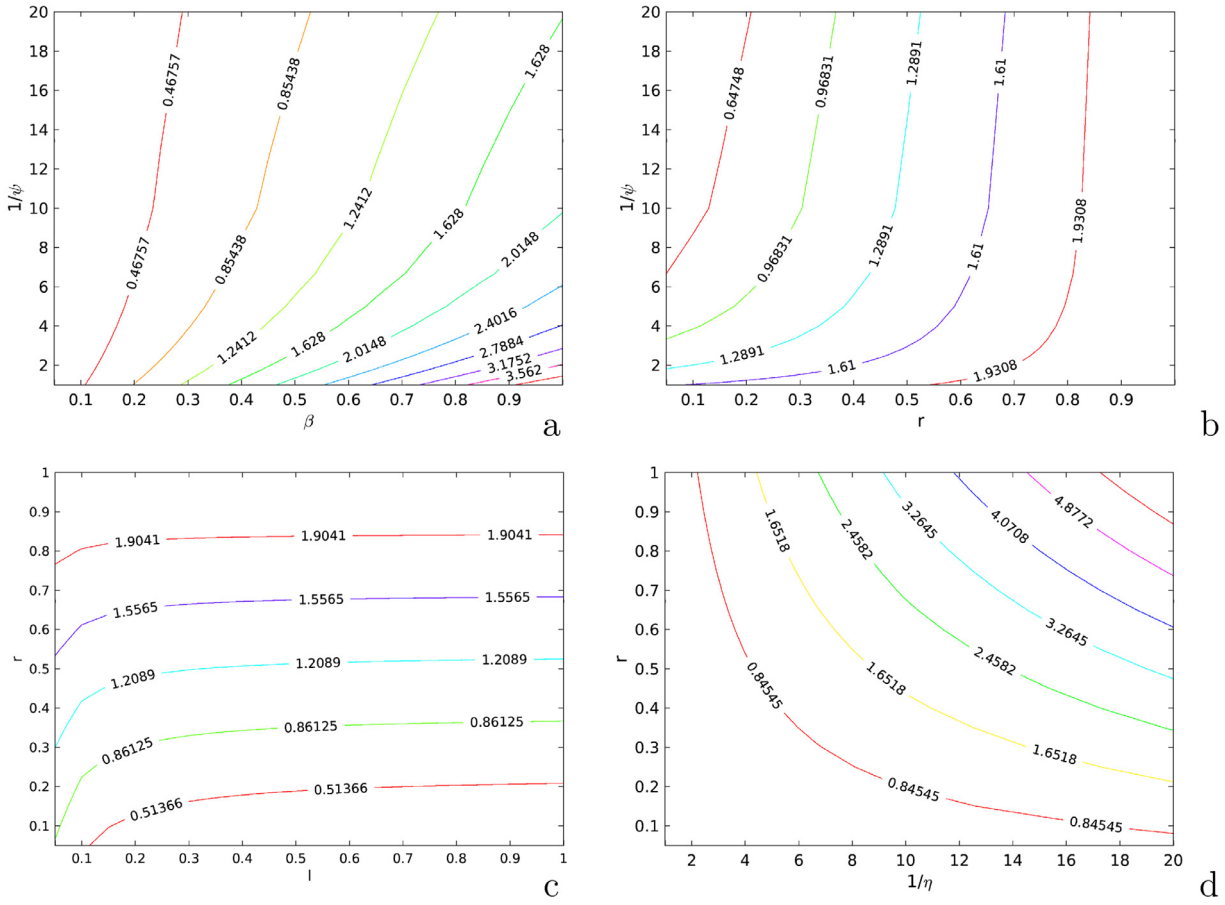

Fig. 8. Contour plots of R_0 versus (a) lockdown period and transmission rate, (b) lockdown period and lockdown efficacy, (c) lockdown efficacy and lockdown success rate, (d) lockdown efficacy and the number of days spent in the infectious period until hospitalized for India. All parameter values are given in Tables 1 and 2.

Therefore by combining all above equations, it follows that each solution of the model Eq. (2.1), with initial conditions $\in \Omega$, approaches ε_0 as $t \to \infty$ for $R_0^* \leq \theta < 1$. □

The above result shows that, for the case when the lockdown efficacy in preventing infection is perfect (i.e., $r = 0$), the disease can be eliminated from the community if the associated reproduction number of the model is less than unity. Furthermore, this result clearly shows that the backward bifurcation property of the model (2.1) is caused by the imperfect nature of the lockdown efficacy to prevent infection.

4. Model calibration and COVID-19 data source

Daily COVID-19 reported cases India for the time period March, 14th 2020 to April, 19th 2020, Mexico for the time period March, 26th 2020 to July, 9th 2020, South Africa for the time period March, 17th 2020 to July, 9th 2020 and Argentina for the time period March, 14th 2020 to July, 9th 2020 are considered for our study. Daily COVID-19 notified cases were collected from [26] for India and from [13] for Mexico, South Africa and Argentina. We fit the model (2.1) to daily new hospitalized cases of COVID for these four countries. The notified cases are hospitalized immediately due to the high transmissibility, and thus it is convenient to fit the hospitalized cases to the reported data. We have mentioned the key parameters of the model (2.1) that are estimated from the data in Table 1. We estimate four unknown model parameters such as: (a) the transmission rate of infected individuals (β), (b) incubation period ($\frac{1}{\gamma}$), (c) rate at which symptomatic infected become hospitalized or notified (η) and (d) recovery rate for symptomatic infected (τ_1) by fitting the model to the newly daily reported cases. Some unknown initial conditions of the model (2.1) also be emitimated from the data. During the specified time period, nonlinear least square solver *fmincon* is used to fit simulated newly daily data in MATLAB reported by COVID-19 for India, Mexico, South Africa and Argentina. We used Delayed Rejection Adaptive Metropolis algorithm [34] to generate the 95% confidence region. An explanation of this technique for model fitting is given in [35]. The estimated parameters are given in Table 2 the estimated values of unknown initial conditions are given by Table 3. The fitting of the daily new hospitalized COVID cases of this four country are displayed in Fig. 4. Using these estimated parameters from Table 2 and the fixed parameters from Table 4, we calculate the basic reproduction numbers given in Table 5.

5. Short-term prediction of COVID-19 cases

The short-term prediction of the model (2.1) is discussed in this section. We simulate the newly hospitalized cases of COVID-19 for the period March 14, 2020 to May 21, 2020 for India using estimated parameters from Table 2. All other fixed parameters are taken from Table 4. The prediction for India in the short term is shown in Fig. 5. The official lockdown period is declared by India Government is from March 25, 2020 to May 3, 2020. For that we have predicted our model for the time period from March 14, 2020 to March 24, 2020 without lockdown. After that we predict our model for the time period March 25, 2020 to May 3, 2020 with lockdown and finally we predict our model for the time period May 4, 2020 to May 21, 2020 without lockdown. We have

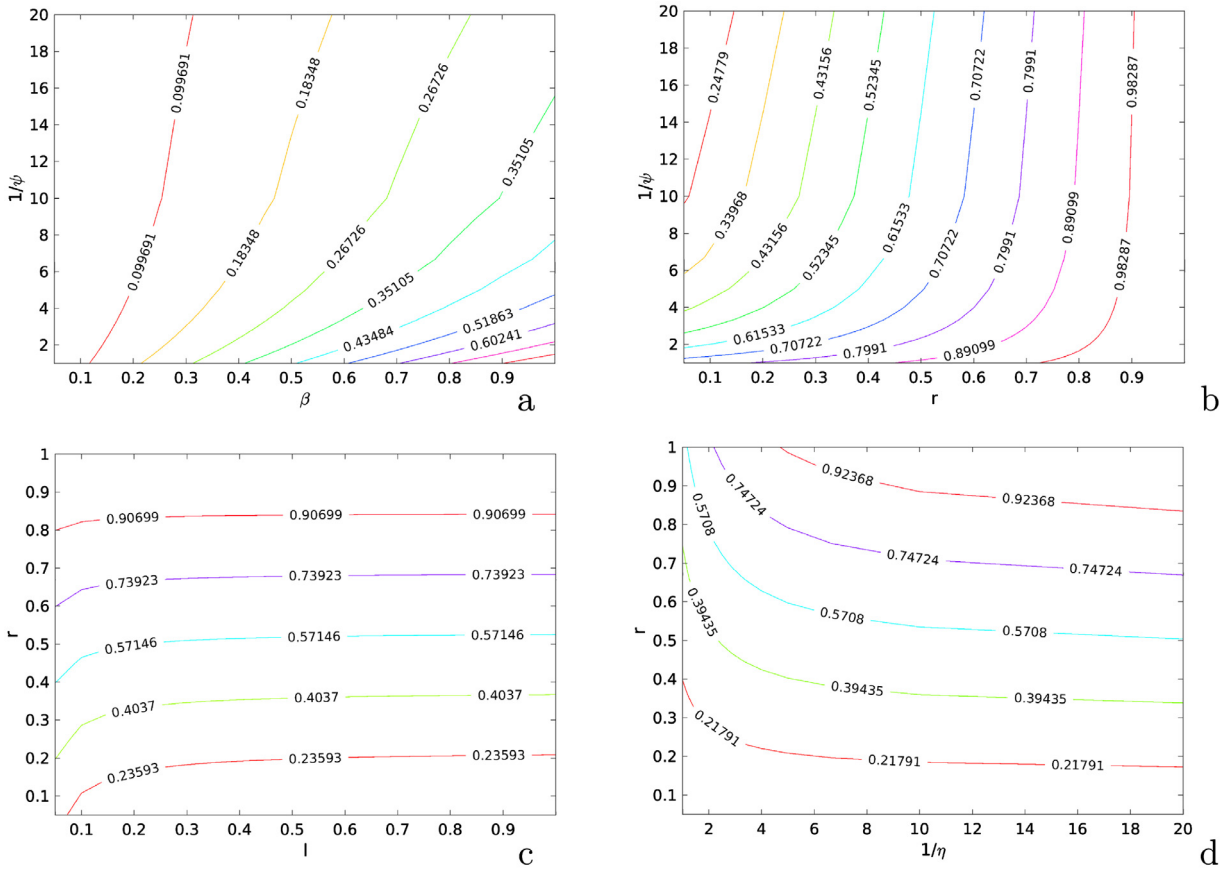

Fig. 9. Contour plots of R_0 versus (a) lockdown period and transmission rate, (b) lockdown period and lockdown efficacy, (c) lockdown efficacy and lockdown success rate, (d) lockdown efficacy and the number of days spent in the infectious period until hospitalized for Mexico. All parameter values are given in Tables 1 and 2.

seen that our prediction is to be pretty good for actual data till now. From the prediction, we find that the COVID-19 cases are going to decrease at the end of the lockdown period. But when the lockdown ends, cases again grow rapidly after few days. Also we have predict our model for the time period from March 26, 2020 to July 19, 2020 for Mexico, from March 17, 2020 to July 19, 2020 for South Africa and from March 14, 2020 to July 19, 2020 for Argentina in the lockdown period and post lockdown period. In this case our prediction is to be pretty good for actual data. For Mexico and Argentina, cases increase very rapidly in the lockdown and post-lockdown period. In South Africa, the lockdown period is only 35 days and cases increase slowly during the lockdown period. But after the lockdown time, cases massively increase. So lockdown is not much effective in Mexico and Argentina while effective lockdown is very important to reduce disease burden in South Africa.

6. Effect of lockdown and control strategies

In this section, the impact of lockdown is measured qualitatively on the disease transmission dynamics. A threshold study of the parameters correlated with the lockdown of susceptible individuals l is performed by measuring the partial derivatives of the basic reproduction number R_0 with respect to this parameters. We observe that

$$\frac{\partial R_0}{\partial l} = -\frac{(1-r)\beta\gamma(\mu+\psi)}{(\gamma+\mu)(\eta+\tau_1+\mu)(\mu+\psi+l)^2} \tag{6.1}$$

so that $\frac{\partial R_0}{\partial l} < 0$ for all $0 < r < 1$.

From this analysis, we have seen that the lockdown efficacy have always positive population-level impact. That means, for every value of lockdown efficacy (r), the lockdown of susceptible individuals results in a reduction of the basic reproduction number R_0 and therefore reduction of the disease burden. The result is summarized in the following lemma:

Lemma 6.1. *For the model (2.1), the impact of lockdown of susceptible individuals will have always positive population-level impact for every* $0 < r < 1$.

The basic reproduction number R_0 is a decreasing function with respect to the lockdown success rate l irrespective of the value of r. We simulate the model for India, Mexico, South Africa and Argentina, in which the results are compatible with the empirical findings discussed above which is displayed in Fig. 6 for India (see the Fig. 13 in **Appendix A** for Mexico(MEX), South Africa(SA) and Argentina(ARG)).

From Fig. 6 (and Fig. 13 in **Appendix A**), it is clear that lockdown success rate l has always positive population-level impact that means R_0 decreases by increasing the value of l for different value of r. We have seen that whenever r=1, the basic reproduction number become constant and for $0 < r < 1$, the population-level impact is always positive. This result indicate that lockdown programs always should run effectivly.

We perform the sensitivity of model parameters with respect to the significant response variable and analyze different control parameters to limit COVID cases for the four countries. In order to get an overview of most influential parameters, we compute the normalized forward sensitivity indices of the model parameters with respect to basic reproduction number R_0. We have chosen parameters transmission rate between human population β, rate of transition from exposed to infected class γ, the rate at which symp-

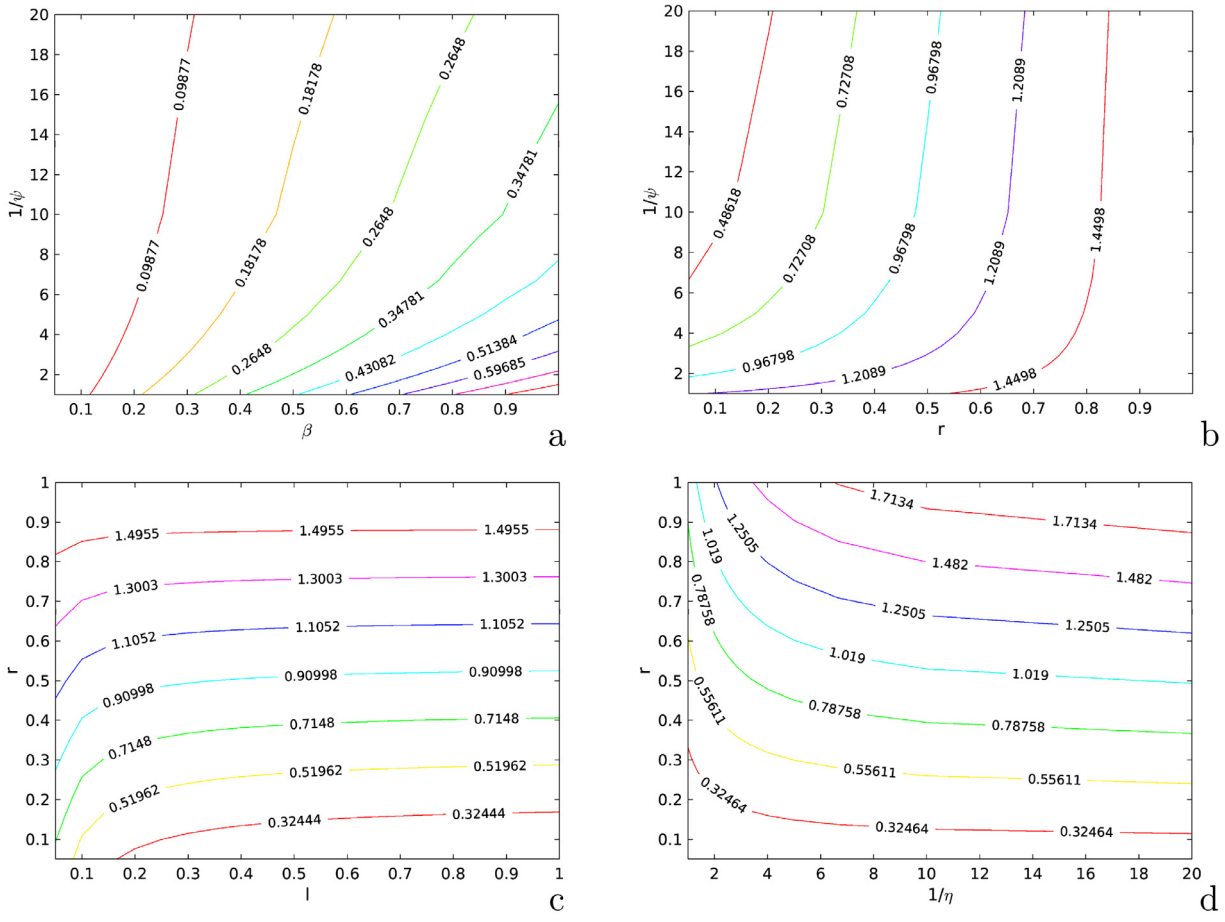

Fig. 10. Contour plots of R_0 versus (a) lockdown period and transmission rate, (b) lockdown period and lockdown efficacy, (c) lockdown efficacy and lockdown success rate, (d) lockdown efficacy and the number of days spent in the infectious period until hospitalized for South Africa. All parameter values are given in Tables 1 and 2.

tomatic infected become hospitalized or notified η, recovery rate for symptomatic infected τ_1, lockdown success rate l and lockdown efficacy r for sensitivity analysis. We use the estimated parameters from Table 2 for the baseline values. The rest of the parameter values are the same as in Table 4. The bar diagram of the normalized forward sensitivity values of R_0 against these parameters is depicted in Fig. 7. However, the mathematical definition of the normalized forward sensitivity index of a variable m with respect to a parameter τ (where m depends explicitly on the parameter τ) is given as:

$$X_m^\tau = \frac{\partial m}{\partial \tau} \times \frac{\tau}{m}.$$

The normalized forward sensitivity indices of R_0 with respect to the parameters β, η, l and r for India are found to be

$$X_{R_0}^\beta = 1, X_{R_0}^\eta = -0.9415, X_{R_0}^l = -0.3418, X_{R_0}^r = 0.6094.$$

The fact that $X_{R_0}^\beta = 1$, means that if we increase 1% in β, keeping other parameters be fixed, will produce 1% increase in R_0. Similarly, $X_{R_0}^\eta = -0.9415$ means increasing the parameter η by 1%, the value of R_0 will be decrease by 0.9415% keeping the value of other parameters be fixed. Therefore, the transmission rate between susceptible humans and lockdown efficacy is positively correlated. On the other hand rate at which symptomatic infected become hospitalized or notified and lockdown success rate is negatively correlated with respect to basic reproduction number. The sensitivity indices of R_0 with respect to the parameters β, η, l and r for Mexico, South Africa and Argentina are given in the Table 6. We have seen that the transmission rate between susceptible humans and lockdown efficacy is positively correlated and the recovery rate of symptomatic infected and lockdown success rate is negatively correlated with respect to basic reproduction number.

In addition, we draw the contour plots of R_0 with respect to the different parameters for the model (2.1) to investigate the effect of the control parameters on basic reproduction number R_0. We have seen a similar patteren for this four countries.

In cases India, the contour plots in Fig. 8 show the dependence of R_0 on different parameters. In Fig. 8(a) and (b), the contours show that increasing the lockdown period reduces the amount of basic reproduction number and, therefore, COVID cases, but increasing the transmission rate and lockdown efficacy increases the basic reproduction number R_0. Furthermore in Fig. 8(c) and (d), we have seen that increasing the lockdown efficacy (r) increases the basic reproduction number. Further increasing the lockdown success rate decreases the basic reproduction number and increasing the number of infectious days increases the basic reproduction number R_0.

For Mexico, South Africa and Argentina, we have seen a similar patteren as India. The contour plots in Figs. 9–11 show the dependence of R_0 on different parameters for this three countries. In Figs. 9(a), 10(a), 11(a) and Figs. 9(b), 10(b), 11(b), the contours show that increasing the lockdown period reduces the amount of basic reproduction number but increasing the transmission rate and lockdown efficacy increases the basic reproduction number R_0 respectively. In Figs. 9(c), 10(c), 11(c) and Figs. 9(d), 10(d), 11(d), we have seen that increasing the lockdown efficacy (r) increases the basic reproduction number respectively. Further increasing the lockdown success rate decreases the basic reproduction number

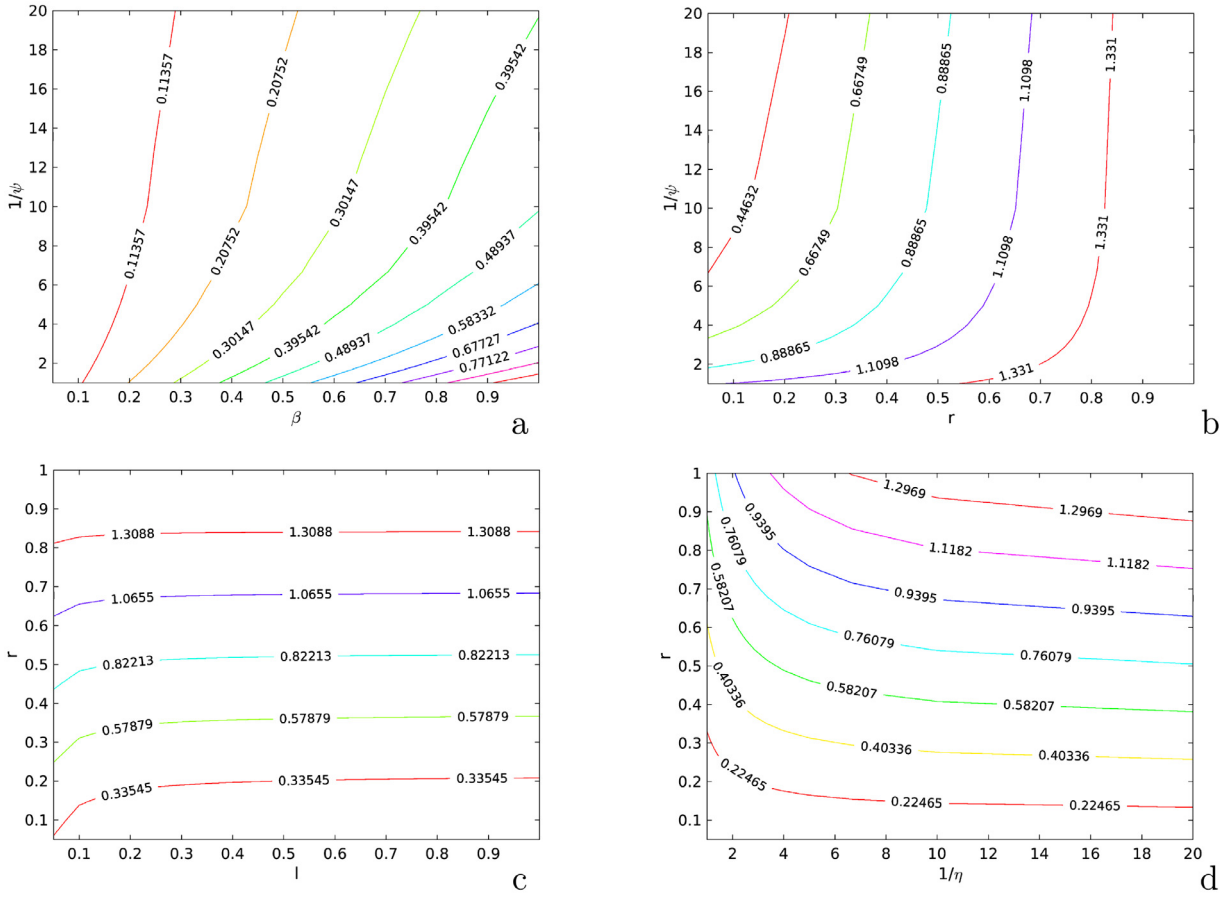

Fig. 11. Contour plots of R_0 versus (a) lockdown period and transmission rate, (b) lockdown period and lockdown efficacy, (c) lockdown efficacy and lockdown success rate, (d) lockdown efficacy and the number of days spent in the infectious period until hospitalized for Argrntina. All parameter values are given in Tables 1 and 2.

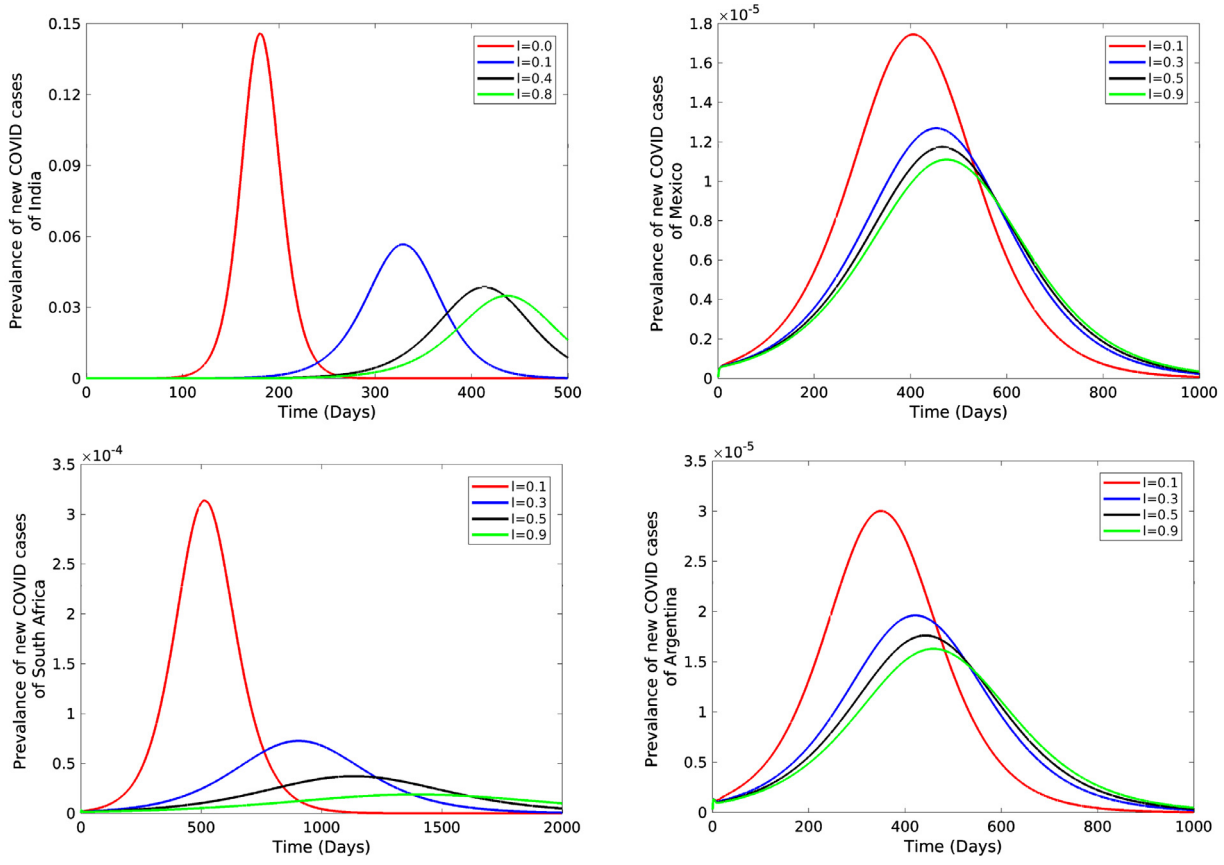

Fig. 12. Effect of lockdown on the prevalence of new COVID-19 cases for different lockdown success rate *l*.

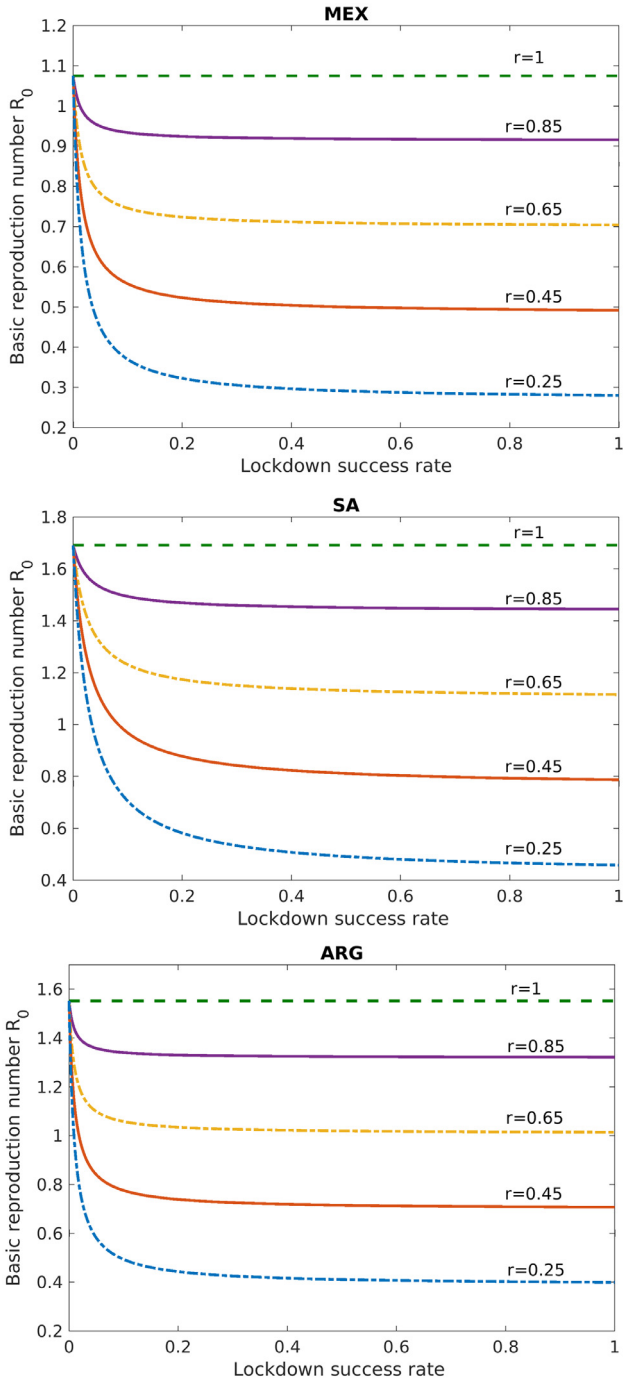

Fig. 13. Effect of lockdown success rate l on basic reproduction number R_0.

and increasing the number of infectious days increases the basic reproduction number R_0.

From the above finding it follows that lockdown success rate and lockdown efficacy is very important to control the diseases. This control can be obtained by an extension of the lockdown period during the outbreak.

For different lockdown success rates, we investigated the impact of lockdown on the prevalence of new COVID-19 cases. The prevalence here is a fraction of individuals in a given particular class. For example, the prevalence of J means "J/Total population". Numerical simulations show that increasing the success rate for lockdowns (l), the prevalence of new COVID cases decreases as the lower value of l increases the prevalence quickly and decreases faster than the higher value of l for India and South Africa(See the Fig. 12). This means that although it is a slow process, the lockdown is very effective in reducing the risk of disease burden. But the numerical simulations revealed that increasing the success rate for lockdowns (l), the prevalence of new COVID cases decreases slowly for Mexico and Argentina. In that case we have seen that in the lower value of l and in higher value of l, the prevalence decreases after a certain time point which is very slow(See the Fig. 12). That means extension of lockdown for these two countries is not too much effective.

7. Discussion and conclusion

This paper provides a deterministic model for the transmission dynamics of COVID-19 outbreak. The model, which adopts standard incidence functions in a realistic way, allows COVID-19 to be transmitted by unnotified individuals. On COVID-19 transmission, we consider the mathematical model with the imperfect lockdown effect. To gain insight into its dynamic features, the model was rigorously analyzed. The findings obtained are as follows. The basic reproduction number for the proposed model is calculated using the next-generation matrix method. The model has a locally-stable disease-free equilibrium whenever the basic reproduction number is less than unity. A detailed study of the model, based on the use of center manifold theory, reveals the existence of the backward bifurcation phenomenon, where two stable equilibria, namely the disease-free equilibrium and an endemic equilibrium coexist when the corresponding basic number of reproduction is less than unity. This backward bifurcation phenomena of this study is very important, and this occurs only under imperfect lockdown individuals. This is basically telling us even if the basic reproduction number is less than one, but the disease will persists which is against classical epidemiological theory. In such a situation, the policy makers may stop surveillance, and the results will be disaster. Our model exhibits the non-existence of backward bifurcation when the lockdown is perfect ($r = 0$). We have seen that the disease-free equilibrium is globally asymptotically stable whenever the associated basic reproduction number is less than unity for the perfect lockdown model. This result indicates that the backward bifurcation property of the model (2.1) is caused by the imperfect nature of the lockdown efficacy to prevent infection. However this backward bifurcation phenomenon is not new in the epidemic model as this phenomenon studied in many previous epidemic models. Furthermore, we calibrated the proposed model to fit India's daily data during the time period of March 14th, 2020 to April 19th, 2020. We also calibrated the model parameters to daily data of Mexico, South Africa and Argentina for a certain time period. We provided a short-term prediction for India, Mexico, South Africa and Argentina of future cases of COVID-19 using the estimated parameters. We have seen that our prediction is to be pretty good for actual data till now. From the prediction, we find that the COVID-19 cases in India are going to decrease at the end of the lockdown period. But when the lockdown ends, cases again grow rapidly after few days. From this finding it follows that lockdown is not sufficient for the given time period as the cases increases after the lockdown ends. Also from the prediction, we find that the COVID-19 cases in Mexico and South Africa are also going to increase at the end of the lockdown period and post lockdown period as the lockdown period is very small in Mexico and South Africa. Though the lockdown period is 101 days in Argentina but the cases increase in both lockdown and post lockdown period. From this finding it follows that lockdown is not sufficient for the given time period as the cases increases after the lockdown ends. We calculate the basic reproduction numbers for the mentioned four countries using the estimated parameter. We study the impact of lockdown in different scenario. From the Fig. 6 it is observed that increasing

the lockdown success rate reduces the basic reproduction number irrespective of the value of lockdown efficacy r. It is clear that lockdown success rate l has always positive population-level impact (R_0 decreases with an increase in l). This result indicates that lockdown programs always should run effectively to control the outbreak. Sensitivity analysis shows that the rate of transmission and lockdown efficacy is positively correlated and the rate at which symptomatic infected individuals are hospitalized or notified, recovery rate of symptomatic infected and the rate of lockdown success rate is negatively correlated with the basic reproduction number. The contour plots in Figs. 8–11 show that increasing the lockdown period decreases the basic reproduction number and thus COVID cases. Further we should reduce the lockdown efficacy (r) to control the disease outbreak. We have also found that increasing the lockdown success rate decreases the basic reproduction number and increasing the number of infectious days increases the basic reproduction number R_0. We have also investigated the impact of lockdown on the prevalence of new COVID-19 cases for different lockdown success rate. This finding suggests that for India and South Africa, the lockdown is very effective in reducing the risk of disease burden although it is a slow process. But lockdown is not effective in Mexico and Argentina as the lower and higher value of l, the prevalence decreases after a certain time which is very slow. From the above finding suggest that in between lockdown period, lockdown success rate (l) and lockdown efficacy (r) is very important to control the disease outbreak.

Declaration of Competing Interest

The authors declare that they have no conflicts of interest.

CRediT authorship contribution statement

Sk Shahid Nadim: Conceptualization, Data curation, Formal analysis, Investigation, Methodology, Software, Supervision, Validation, Writing - original draft, Writing - review & editing. **Joydev Chattopadhyay:** Supervision, Writing - original draft, Writing - review & editing.

Acknowledgments

The authors are grateful to the anonymous referees for their careful reading, valuable comments and helpful suggestions, which helped to improve the standard of this work. Sk Shahid Nadim receives funding from Council of Scientific & Industrial Research as senior research fellowship (Grant No. 09/093(0172)/2016/EMR-I), Government of India, New Delhi. The authors would like to thanks Dr Tridip Sardar for his valuable suggestions.

Appendix A

The center manifold theory [32,36] is used to determine the existence of the backward bifurcation phenomenon of the model (2.1) theoretically.

Theorem A.1. *Let us consider the following general system of ordinary differential equations with a parameter* ϕ

$$\frac{dx}{dt} = f(x, \phi),\ f : R^n \times R \to R^n,\ f \in C^2(R^n \times R) \tag{A-1}$$

Without loss of generality, it is assumed that $x = 0$ *is an equilibrium for system (A-1) for all values of the parameter* ϕ.

Assume that $(1) A = D_x f(0, 0)$ *is the linearized matrix of system (A-1) around the equilibrium* $x = 0$ *with* ϕ *evaluated at 0. Zero is a simple eigenvalues of A and all other eigenvalue of A have negative real parts;*

(2) Matrix A has a nonnegative right eigenvector w and a left eigenvector v corresponding to the zero eigenvalue. Let f_k *be the kth component of f and*

$$a = \sum_{k,i,j=1}^{n} v_k w_i w_j \frac{\partial^2 f_k}{\partial x_i \partial x_j}(0, 0)$$

$$b = \sum_{k,i=1}^{n} v_k w_i \frac{\partial^2 f_k}{\partial x_i \partial \beta}(0, 0)$$

Then, the local dynamics of system (A-1) around 0 are totally determined by the sign of a and b.

(i) $a > 0,\ b > 0$. *When* $\phi < 0$ *with* $|\phi| \ll 1,\ x = 0$ *is locally asymptotically stable and there exists a positive unstable equilibrium; when* $0 < \phi \ll 1,\ x = 0$ *is unstable and there exists a negative and locally asymptotically equilibrium;*

(ii) $a < 0,\ b < 0$. *When* $\phi < 0$, *with* $|\phi| \ll 1,\ x = 0$ *is unstable; when* $0 < \phi \ll 1,\ x = 0$ *is locally asymptotically stable and there exists a negative unstable equilibrium;*

(iii) $a > 0,\ b < 0$. *When* $\phi < 0$, *with* $|\phi| \ll 1,\ x = 0$ *is unstable and there exists a locally asymptotically stable negative equilibrium; when* $0 < \phi \ll 1,\ x = 0$ *is stable and a positive unstable equilibrium appears;*

(iv) $a < 0,\ b > 0$. *When* ϕ *changes from negative to positive,* $x = 0$ *changes its stability from stable to unstable. Correspondingly, a negative unstable equilibrium becomes positive and locally asymptotically stable.*

In particular, if $a > 0,\ b > 0$ *then a backward bifurcation occurs at* $\phi = 0$.

References

[1] Who. Coronavirus disease 2019 (COVID-19).https://www.who.int/emergencies/diseases/novel-coronavirus-2019/situation-reports; 2020. Retrieved : 2020-04-23.
[2] Chen Y, Liu Q, Guo D. Emerging coronaviruses: genome structure, replication, and pathogenesis. J Med Virol 2020;92(4):418–23.
[3] Tang B, Wang X, Li Q, Bragazzi NL, Tang S, Xiao Y, et al. Estimation of the transmission risk of the 2019-nCoV and its implication for public health interventions. J Clin Med 2020;9(2):462.
[4] Gralinski LE, Menachery VD. Return of the coronavirus: 2019-nCoV. Viruses 2020;12(2):135.
[5] Huang C, Wang Y, Li X, Ren L, Zhao J, Hu Y, et al. Clinical features of patients infected with 2019 novel coronavirus in Wuhan, China. Lancet 2020;395(10223):497–506.
[6] Hui DS, Azhar EI, Madani TA, Ntoumi F, Kock R, Dar O, et al. The continuing 2019-nCoV epidemic threat of novel coronaviruses to global health – the latest 2019 novel coronavirus outbreak in Wuhan, China. Int J Infect Dis 2020;91:264.
[7] Thompson R. Pandemic potential of 2019-nCoV. Lancet Infect Dis 2020;20(3):280.
[8] Li W, Moore MJ, Vasilieva N, Sui J, Wong SK, Berne MA, et al. Angiotensin–converting enzyme 2 is a functional receptor for the SARS coronavirus. Nature 2003;426(6965):450–4.
[9] de Wit E, van Doremalen N, Falzarano D, Munster VJ. SARS and MERS: recent insights into emerging coronaviruses. Nat Rev Microbiol 2016;14(8):523.
[10] Cowling BJ, Park M, Fang VJ, Wu P, Leung GM, Wu JT. Preliminary epidemiologic assessment of MERS-Cov outbreak in South Korea, May–June 2015. Euro Surveill 2015;20(25).
[11] Indias coronavirus lockdown. https://www.vox.com/2020/3/24/21190868/coronavirus-india-modi-lockdown-kashmir; 2020. Retrieved : 2020-04-23.
[12] Mohfw, Coronavirus disease 2019 (COVID-19).https://www.mohfw.gov.in/; 2020. Retrieved : 2020-04-23.
[13] India demographics. https://www.worldometers.info/world-population/india-population/; 2020. Retrieved : 2020-04-03.
[14] Kucharski AJ, Russell TW, Diamond C, Liu Y, Edmunds J, Funk S, et al. Early dynamics of transmission and control of COVID-19: a mathematical modelling study. Lancet Infect Dis 2020.
[15] Nadim S.S., Ghosh I., Chattopadhyay J.. Short-term predictions and prevention strategies for COVID-2019: a model based study. arXiv:200308150 2020;.
[16] Sardar T, Nadim SS, Rana S, Chattopadhyay J. Assessment of lockdown effect in some states and overall India: a predictive mathematical study on COVID-19 outbreak. Chaos Solitons Fractals 2020:110078.
[17] Senapati A., Rana S., Das T., Chattopadhyay J.. Impact of intervention on the spread of COVID-19 in India: a model based study. arXiv:200404950 2020;.
[18] Zhao S, Lin Q, Ran J, Musa SS, Yang G, Wang W, et al. Preliminary estimation of the basic reproduction number of novel coronavirus (2019-nCoV) in china, from 2019 to 2020: adata-driven analysis in the early phase of the outbreak. Int J Infect Dis 2020;92:214–17.

[19] Zhao S, Musa SS, Lin Q, Ran J, Yang G, Wang W, et al. Estimating the unreported number of novel coronavirus (2019-nCoV) cases in China in the first half of January 2020: a data-driven modelling analysis of the early outbreak. J Clin Med 2020;9(2):388.
[20] Gumel A. Causes of backward bifurcations in some epidemiological models. J Math Anal Appl 2012;395(1):355–65.
[21] Garba SM, Gumel AB, Bakar MA. Backward bifurcations in dengue transmission dynamics. Math Biosci 2008;215(1):11–25.
[22] Singer BH, Kirschner DE. Influence of backward bifurcation on interpretation of r_0 in a model of epidemic tuberculosis with reinfection. Math Biosci Eng 2004;1(1):81.
[23] Zhang X, Liu X. Backward bifurcation of an epidemic model with saturated treatment function. J Math Anal Appl 2008;348(1):433–43.
[24] Diekmann O, Heesterbeek JAP. Mathematical epidemiology of infectious diseases: model building, analysis and interpretation, vol 5. John Wiley & Sons; 2000.
[25] Hethcote HW. The mathematics of infectious diseases. SIAM Rev 2000;42(4):599–653.
[26] India COVID-19 tracker.https://www.covid19india.org/; 2020. Retrieved : 2020-04-03.
[27] COVID-19 pandemic lockdowns. https://en.wikipedia.org/wiki/COVID-19_pandemic_lockdowns; 2020. Retrieved : 2020-07-09.
[28] Thieme H.. Mathematics in population biology2003;.
[29] Smith HL, Waltman P. The theory of the chemostat: dynamics of microbial competition, vol 13. Cambridge university press; 1995.
[30] Diekmann O, Heesterbeek JAP, Metz JA. On the definition and the computation of the basic reproduction ratio r 0 in models for infectious diseases in heterogeneous populations. J Math Biol 1990;28(4):365–82.
[31] Van den Driessche P, Watmough J. Reproduction numbers and sub-threshold endemic equilibria for compartmental models of disease transmission. Math Biosci 2002;180(1–2):29–48.
[32] Castillo-Chavez C, Song B. Dynamical models of tuberculosis and their applications. Math Biosci Eng 2004;1(2):361.
[33] LaSalle JP. The stability of dynamical systems, vol 25. Siam; 1976.
[34] Haario H, Laine M, Mira A, Saksman E. DRAM: efficient adaptive MCMC. Stat Comput 2006;16(4):339–54.
[35] Sardar T, Saha B. Mathematical analysis of a power-law form time dependent vector-borne disease transmission model. Math Biosci 2017;288:109–23.
[36] Carr J. Applications of centre manifold theory, vol 35. Springer Science & Business Media; 2012.